ISSN 1674-1056
http://cpb.iphy.ac.cn
http://iopscience.iop.org/cpb
中国物理 B
Chinese Physics
中国物理 Chinese Physics B

Application of millimeter-sized polymer cylindrical lens array concentrators in solar cells

Yao-Ju Zhang(张耀举), Yi-Jie Li(李艺杰), Jie Lin(林洁), Chao-Long Fang(方朝龙), Si-Yuan Liu(刘思远)
Citation: Chin. Phys. B . 2018, 27(5): 058801. **doi:** 10.1088/1674-1056/27/5/058801

Journal homepage: http://cpb.iphy.ac.cn; http://iopscience.iop.org/cpb

What follows is a list of articles you may be interested in

Importance of PbI_2 morphology in two-step deposition of $CH_3NH_3PbI_3$ for high-performance perovskite solar cells

Hui Wei(韦慧), Yang Tang(汤洋), Bo Feng(冯波), Hui You(尤晖)
Chin. Phys. B . 2017, 26(12): 128801. **doi:** 10.1088/1674-1056/26/12/128801

Improvement in IBC-silicon solar cell performance by insertion of highly doped crystalline layer at heterojunction interfaces

Hadi Bashiri, Mohammad Azim Karami, Shahramm Mohammadnejad
Chin. Phys. B . 2017, 26(10): 108801. **doi:** 10.1088/1674-1056/26/10/108801

Comparision between Ga- and N-polarity InGaN solar cells with gradient-In-composition intrinsic layers

Lin Lu(鲁麟), Ming-Chao Li(李明潮), Chen Lv(吕琛), Wen-Gen Gao(高文根), Ming Jiang(江明), Fu-Jun Xu(许福军), Qi-Gong Chen(陈其工)
Chin. Phys. B . 2016, 25(10): 108801. **doi:** 10.1088/1674-1056/25/10/108801

Effects of polarization and p-type GaN resistivity on the spectral response of InGaN/GaN multiple quantum well solar cells

Yang Jing, Zhao De-Gang, Jiang De-Sheng, Liu Zong-Shun, Chen Ping, Li Liang, Wu Liang-Liang, Le Ling-Cong, Li Xiao-Jing, He Xiao-Guang, Wang Hui, Zhu Jian-Jun, Zhang Shu-Ming, Zhang Bao-Shun, Yang Hui
Chin. Phys. B . 2014, 23(6): 068801. **doi:** 10.1088/1674-1056/23/6/068801

β-$FeSi_2$ as the bottom absorber of triple-junction thin-film solar cells：A numerical study

Yuan Ji-Ren, Shen Hong-Lie, Zhou Lang, Huang Hai-Bin, Zhou Nai-Gen, Deng Xin-Hua, Yu Qi-Ming
Chin. Phys. B . 2014, 23(3): 038801. **doi:** 10.1088/1674-1056/23/3/038801

Application of millimeter-sized polymer cylindrical lens array concentrators in solar cells*

Yao-Ju Zhang(张耀举)†, Yi-Jie Li(李艺杰), Jie Lin(林洁),
Chao-Long Fang(方朝龙)‡, and Si-Yuan Liu(刘思远)

College of Physics and Electronic Information Engineering, Wenzhou University, Wenzhou 325035, *China*

(Received 6 February 2018; published online 26 April 2018)

A unique method is proposed to encapsulate solar cells and improve their power conversion efficiency by using a millimeter-sized cylindrical lens array concentrator. Millimeter-sized epoxy resin polymer (ERP) cylindrical lens array concentrators are fabricated by the soft imprint technique based on polydimethylsiloxane stamps. The photovoltaic measurements show that millimeter-sized ERP cylindrical lens array concentrators can considerably improve the power conversion efficiency of silicon solar cells. The validity of the proposed method is proved by the coupled optical and electrical simulations. The designed solar cell devices with the advantages of high-efficiency and convenient cleaning are very useful in practical applications.

Keywords: millimeter-sized cylindrical array concentrator, silicon solar cells, high-efficiency, soft imprint method

PACS: 88.40.hj, 88.40.fr, 42.79.Ek **DOI:** 10.1088/1674-1056/27/5/058801

1. Introduction

Photovoltaic (PV) technology is considered to be one of the most promising alternatives to fossil fuels, as it provides a source of energy that is both sustainable and environmentally friendly. The PV market has experienced a rapid growth over the past two decades.[1–4] The crystalline silicon (c-Si) solar cell, which was over 90% of the market in 2014,[2] represents a cost effective, environment-friendly, and proven renewable energy resource. Industrially manufacturing of c-Si solar cell has now matured in terms of efficiency and cost. Wafer-based c-Si solar cells are produced from slices of either single-crystal silicon (sc-Si) or multi-crystalline silicon (mc-Si), boosting a market share of 35% or 55% respectively in 2014.[2] On the other hand, since technology advances and government-oriented policy support through feed-in tariffs,[1,4] the price of silicon PV cells has decreased from $76 per watt in 1977 to $0.3 per watt at present.

One of greatest technology advances in c-Si PV technology is the textured structure of silicon solar cell, which is useful in improving the efficiency of solar cells. Ideally, a solar cell should absorb all useful photons. However, more than 33% of incident light is reflected back from the flat surface of c-Si solar cells. The surface of silicon in current high-efficiency c-Si solar cells has a complex surface structure such as pyramid,[5,6] inverted pyramid,[7–9] biomimetic,[10] subwavelength grating,[11–14] nanowire array,[15–17] and other nano/microstructure.[15,18–20] The micro/nano structure surface of Si PV layer needs to be permanently protected by encapsulation, for providing and maintaining a transparent physical isolation from the exterior environment.[21,22] The plane protective transparent film encapsulation is generally unable to substantially improve the photoelectric conversion efficiency of solar cells.[23,24] Many researches have focused on the improving efficiency of Si solar cells encapsulated by antireflective coating (AR) with complex micro/nanostructure surface.[25–29] It is well known that dust accumulation is one of the natural phenomena, which adversely affects the performance of solar cell devices.[30] Therefore, the surface of solar cell device has to be cleaned termly to maintain the solar cell performance undegraded. Micro/nanostructures are fragile and vulnerable in cleaning the dust particles, which might lead to the serious degradation of the micro/nanostructures AR performance and lower the output power of solar cell device. On the other hand, the fabrication process of the micro/nanostructure AR coatings is complex and the cost of fabrication is high,[25–29,31] which is incompatible with industrial mass production of solar cells.

In order to overcome the disadvantages of micro/nanostructure AR coatings and enhance the application ability of solar cell devices outdoors, we propose the millimeter-sized cylindrical array concentrator to encapsulate Si solar cells. The transparent epoxy resin polymer (ERP), which has a high light transmittance of 92% more in 350–1800 nm solar PV wavelength range and strong stiffness (Yung's modulus is 3.43 GPa),[32,33] is chosen as experimental material of fabricating millimeter-sized cylindrical array concentrators, for lowering the cost in this experiment. Fur-

*Project supported by the Natural National Science Foundation of China (Grant No. 61377021).
†Corresponding author. E-mail: zhangyj@wzu.edu.cn
‡Corresponding author. E-mail: fansy21@163.com
© 2018 Chinese Physical Society and IOP Publishing Ltd

thermore, a milli-scale pattern of template can be facilely transferred to ERP film by using a simple soft stamp method, which has been used in our previous paper.[34] The millimeter-sized ERP cylindrical array concentrators are fabricated by the two-step soft imprint stamp method and their effectiveness in improving the power conversion efficiency (PCE) of solar cells is measured and analyzed by the optical and electrical simulations. The theoretical and experimental results show that the absorptivity of PV Si layer increases and consequently the PCE of solar cells encapsulated by the ERP array concentrator is substantively improved.

2. Experimental and simulation modeling details

2.1. Experiments

Figure 1 shows the schematic diagram illustrating the fabrication procedure of a milimeter-sized cylindrical array concentrator of the ERP film and the encapsulation procedure of the mc-Si solar cell. In process 1 of Fig. 1, to fabricate polydimethylsiloxane (PDMS) stamps with cylindrical concave lens array, the silica glass master mold with cylindrical plano-convex lenses consisting of periodic pattern array was used. The silica glass mold was formed by gluing cylindrical plano-convex lenses side by side. The curvature radius and bottom width of the silica glass cylindrical plano-convex lens were 2.5 mm and 4 mm respectively in the experiment. In consideration of the purchased solar cell with the 2 mm spacing between finger electrodes, we purchased the cylindrical convex lenses with 4 mm in width from the business company (Lianyungang Haisheng Quartz Tech. Co., China). A PDMS film was employed as the soft imprint stamp due to its excellent formability. The PDMS solution prepared by mixing the prepolymer of Sylgard 184A with the copolymer of Sylgard 184B at a weight ratio of 10:1 was poured on the silica glass mold and then cured at a temperature of 80 °C for 2 h in air. The PDMS film was carefully peeled off from the silica glass mold, creating the PDMS imprint stamp with cylindrical concave lens array pattern. Some bare multicrystalline silicon solar cell sheets with a 20 mm×20 mm area, which were purchased from the business company (Taizhou Zhonglai Photoelectric Tech. Co., China), were cleaned with alcohol and subsequently dried in a flowing nitrogen gas. In process 2, a cleaned bare solar cell sheet was pasted onto a substrate with ethylene vinyl acetate copolymer (EVA) adhesive. The ERP solution, which was prepared by mixing the prepolymer purchased from Shenzhen Jinhua Electronic Materials Co. of China with the copolymer at a weight ratio of 2:1, was poured on the cleaned solar cell inside the container. The PDMS stamp was gentle placed onto the ERP solution and was followed by vacuumizing at 0.1 Pa to expel the air between the PDMS and the ERP. The supporting layer height was controlled to be smaller than the focal length, and the center line of each lens is projected into the middle area between finger electrodes to avoid the shading losses. After 8 h curing at 100 °C, the PDMS stamp was carefully peeled off from the ERP surface and finally an ERP-encapsulated mc-Si solar cell with a cylindrical convex lens array front surface was formed.

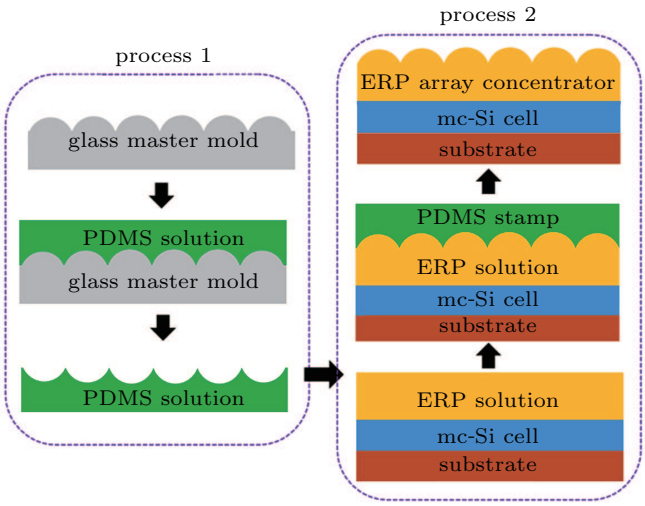


Fig. 1. (color online) Schematic diagram illustrating fabrication procedure of ERP-array-concentrator mc-Si solar cell. Process 1: Fabricating PDMS stamp from glass master mold. Process 2: Fabricating ERP lens array concentrator and encapsulation of the mc-Si solar cell.

2.2. Simulations

For millimeter-sized lens array concentrators, optical simulations were performed by using the rays-trace method in TracePro software.[35] Figure 2 shows the simulation model, where the structure parameters of cylindrical lens are the same as the corresponding parameters indicated in Subsection 2.1. The other structure parameters approximately are those that were used for replicating a realistic mc-Si solar cell, which are presented in Table 1. The refractive indexes of Si (PV layer), SiN (passivation layer), Ag (front contact), and Al (back contact) used in these calculations were cited from the Database in PV lighthouse.[36] The refractive index of the used ERP film was measured by using the ellipsometer (HORIBA UVISEL 2), which is fitted in a range of 350–1200 nm wavelengths as

$$n = 1.5565 + 0.00728035\lambda^{-2} + 0.000221012\lambda^{-4}. \quad (1)$$

In this range of wavelength, the extinction coefficient of the ERP is negligible.[33] The absorption spectra in PV Si layer were obtained from the report of luminous flux in the TracePro, and the absorptivity distribution, $P(\lambda, \boldsymbol{r})$, was obtained from the irradiance map for exiting flux of the observation surface scanned in PV Si layer.

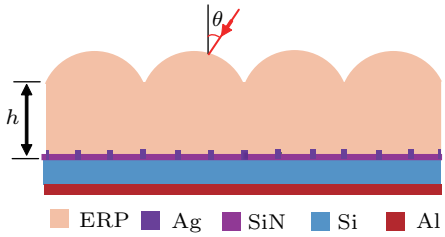


Fig. 2. (color online) Cross-section schematic illustrating ERP-array-concentrator encapsulated mc-Si solar cell structure.

Table 1. Geometry structure parameters of solar cell.

Parameter	Value	Parameter	Value
thickness of Ag	20 μm	thickness of SiN	5 nm
width of Ag	100 μm	height of ERP film	1–4 mm
period of Ag	2 mm	thickness of Al	200 μm
thickness of mc-Si	200 μm		

The coupling with electrical simulations of the solar cell was carried out afterwards by using the finite element method (FEM),[37] which accounts for a wide variety of electronics effects.[38] Continuity equations for electron and hole densities together with the Poisson's equation for the electrostatic potential were solved by the FEM charge simulator. The spatially resolved carrier generation rate $G(\boldsymbol{r})$, calculated from the absorptivity distribution obtained from the TracePro, relates optical simulation to electrical simulation, which is defined as

$$G(\boldsymbol{r}) = \frac{1}{2\hbar}\int_{\lambda_{\min}}^{\lambda_{\max}} \varepsilon_{\mathrm{im}}(\lambda)P(\lambda,\boldsymbol{r})I(\lambda)\,\mathrm{d}\lambda, \qquad (2)$$

where $h = h/2\pi$ with h being the Planck constant, $\varepsilon_{\mathrm{im}}(\lambda)$ is the imaginary part of the permittivity, $\varepsilon_{\mathrm{im}}(\lambda) = 2\varepsilon_0 n(\lambda)\kappa(\lambda)$ with $n(\lambda)$ being the real part of refractive index and $\kappa(\lambda)$ the extinction coefficient of Si, and $\boldsymbol{r}$ denotes the space coordinate. In the FEM charge simulation, Shockley–Read–Hall (SRH) recombination, radiative recombination of carriers, and Auger recombination were considered in PV Si film. In addition to bulk recombination, surface recombinations at three Si–Ag, Si–Al, and Si–SiN interfaces were also taken into account. Table 2 shows the parameters of materials and interfaces and Table 3 shows doping parameters of the solar cell in electrical simulations.

Table 2. Parameters of materials and interfaces.

Parameter and description	value
electron lifetime/s	3.3×10^{-6}
hole lifetime/s	4.0×10^{-6}
electron effective mass (m^*/m_0)	1.18
hole effective mass (m^*/m_0)	0.8098
radiative EHP capture rate/cm^3·s^{-1}	1.6×10^{-14}
electron Auger recombination coefficient/cm^6·s^{-1}	2.8×10^{-31}
hole Auger recombination coefficient/cm^6·s^{-1}	9.8×10^{-31}
Si work function/eV	4.58
Ag work function/eV	4.26
Al work function/eV	4.28
Si permittivity	11.7
SiN permittivity	7.5
electron and hole surface recombination velocity at Si–Al interface/cm·s^{-1}	1.0×10^{9}
electron and hole surface recombination velocity at Si–SiN interface/cm·s^{-1}	1000
electron and hole surface recombination velocity at Si–Ag interface/cm·s^{-1}	1.0×10^{7}
simulation temperature/K	300

Table 1. Doping parameters of solar cell.

Doping region	Type	Concentration	Junction thickness	Thickness	Distribution
background	p	1.5×10^{16} cm^{-3}	–	whole Si	constant
front surface	n	1.0×10^{19} cm^{-3}	0.2 μm	0.3 μm	erfc
back surface	p	1.0×10^{18} cm^{-3}	0.3 μm	0.2 μm	erfc

3. Results and discussion

3.1. Experiment results

Figure 3(a) shows the digital image of the PV performance test system (Keithley 2420+ Newport Class3A solar simulator+ the PVIV software package from Newport). Figure 3(b) shows the measured current density–voltage (J–V) curves of the ERP-encapsulated mc-Si solar cells at $\theta = 0°$ and $h = 3.75$ mm, where θ is the incident angle between incoming sunlight and normal direction of the cell and h is the distance between the lens array and the front surface of the unencapsulated cell. It is found from Fig. 3(b) that the values of open-circuit voltage V_{oc} of two ERP-encapsulated cells with and without the cylindrical lens array concentrator (CLAC) have no significant difference. The short-circuit current density J_{sc} of the solar cell increases from 34.50 mA/cm^2 (without the CLAC) to 37.84 mA/cm^2 (with the CLAC), the improvement rate of J_{sc} being 9.68%, while the filled factor FF decreases from 72.35% to 70.91%, the decrease rate of FF being 1.99%. Since the PCE is proportional to the product of V_{oc}, J_{sc}, and FF, the PCE of the solar cell at $h = 3.75$ mm is improved from 15.33% to 16.45%, the improvement rate being 7.31%. There are two factors which lead to the efficiency improvement of the PV cells with a CLAC. One factor is that the curved surface increases the effective optical path length in PV active layer. The other factor is the focusing function of the cylindrical lens. Under the focusing light incident onto the PV material, the carrier mobility in mc-Si material increases and the recombination of carriers decreases.[39]

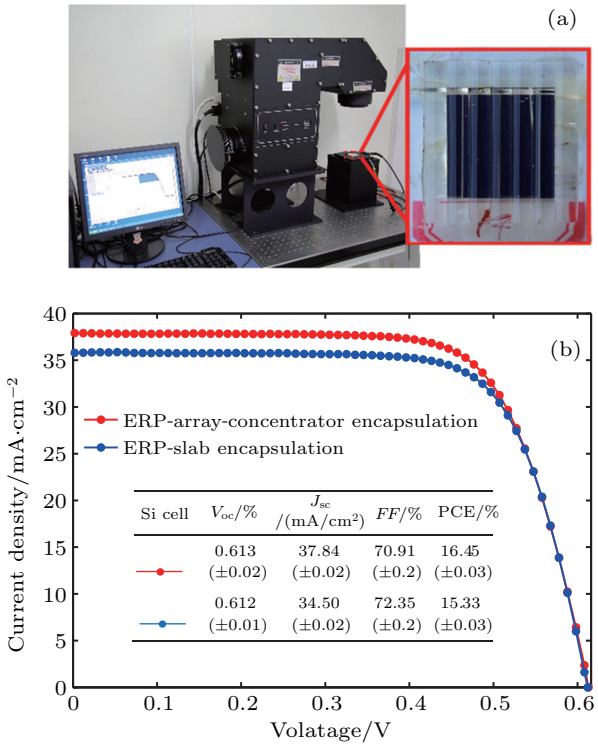


Fig. 3. (color online) (a) Digital image of measurement setup and (b) measured current density–voltage curves of ERP-encapsulated mc-Si cell cells with and without lens array surface at $h = 3.75$ mm and $\theta = 0°$.

Owing to the existence of focusing convex cylindrical lenses in solar cells with the CLAC, the photon utilization efficiency is dependent on the supporting layer height (h). Figure 4 shows the measured PCE improvement of the Si solar cells with the CLAC according to h values ranging from 2.25 mm to 5.25 mm in steps of 0.5 mm. As h increases for small values of $h < 3.75$ mm in Fig. 4, the PCE improvement rate of the solar cell increases, reaching its maximum value of 7.50% at $h = 3.75$ mm with a focusing area ratio of 29.38%. Although the light becomes more focused even with h exceeding 3.75 mm, the PCE of the cell decreases.

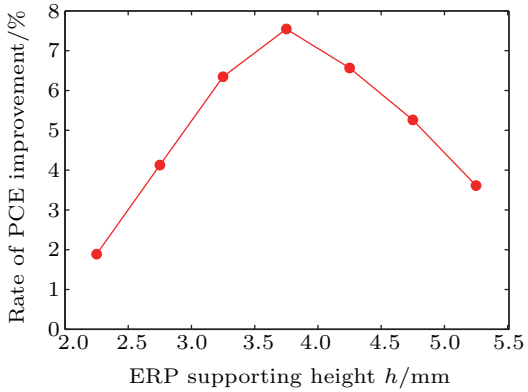


Fig. 4. (color online) Variation of measured rate of PCE improvement with ERP supporting height of the Si solar cell with the CLAC at $\theta = 0°$.

The incident angle of solar radiation is wide due to diffuse light scattered by atmosphere and the positional variations of the sun in a day and the seasons. Thus, the incident light angle-dependent electrical characteristics of the Si PV cells are also important. In order to study the incident angle-dependent performance, the solar cell device is rotated around the axis of cylindrical lens in a θ range of 0°–60° while the solar simulator is fixed in the tests. Figure 5 shows the measured PCE of Si PV solar cells with and without the CLAC. Although the PCE values generally decrease as θ increases, the solar cell with the CLAC exhibits a superior solar energy conversion performance compared with the reference solar cell without the CLAC in two angle ranges of $\theta < 10°$ and $\theta > 23°$. However, it is noted that the PCE of the solar cell with the ERP CLAC is lower than with ERP slab encapsulation in an angle range of 10°–23°. The explanations to this phenomenon are given as follows. When light is incident on the solar cells with the CLAC normally or at a large incident angle, they are focused onto the area between finger electrodes and consequently the PCE of the solar cell is improved due to the focusing effect of lens. Since finger spacings of bought silicon solar cells are fixed, a part of light is probably focused onto finger electrodes when light are incident at an angle of about 10°–23° and consequently the solar cell with the CLAC exhibits a lower PCE than the solar cell without the CLAC. According to the measured data, we calculate the averaged PCE of the solar cell with the CLAC, and the results show that it increased by about 10% (from 13.65% to 15.07%) over a broad θ range of 0°–60°, compared with the averaged PCE of the solar cell without the CLAC. Thus, the use of the array concentrators can lead to the improvement of solar power generation in PV cells in a wide range of incident angle. If an optimised structure of finger electrodes is designed and used in Si solar cells with the CLAC, the shadowing effect can be lowered and the averaged PCE of the solar cell can be further improved, which is of significance for practically deploying the solar panels without using a costly solar tracking system.[40]

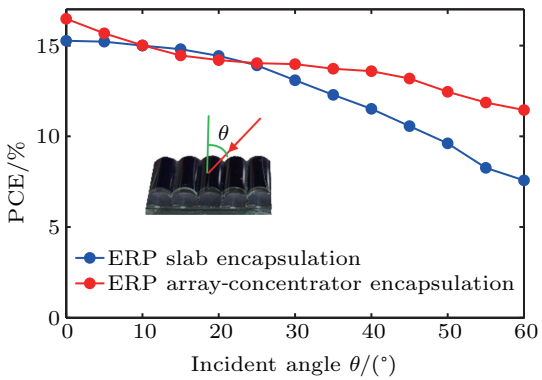


Fig. 5. (color online) Plots of measured PCEs versus incident angle of solar cells encapsulated by the ERP array concentrator and by the ERP slab at $h = 3.75$ mm.

3.2. Simulation results and discussion

In order to explain the experimental results above, we simulate the optical and electrical performance of solar cells by using the optical and electrical simulations, in which the optical absorptivities are calculated by using the TracePro software and the electrical characteristics are simulated by use of the FEM method to solve continuity equations for electron and hole densities together with the Poisson's equation. Figure 6(a) shows the absorption spectra of PV Si layer in solar cells with and without the CLAC when $\theta = 0^\circ$ and $h = 2$ mm. It can be seen that the cylindrical lens array concentrator enhances the optical absorptivity of the PV Si layer in a very wide wavelength range of 350–1100 nm. The integrated absorptivity over 350–1100 nm wavelengths is 58.46% for the Si solar cell with the CLAC, which increases 5.12%, and is larger than 55.61% of the device without the CLAC. Our explanation for this is as follows. For the Si solar cell encapsulated by the ERP slab with specular surfaces, the absorbance in the Si film is equal to $1-\exp(-2\alpha L)$, where α is the optical absorption coefficient of Si, L is the thickness of the Si film, and the factor of 2 accounts for the double pass due to the reflecting rear surface. For the ERP-lens-array-encapsulated Si solar cell with the periodically curved top surface, normally incident light is deflected away from the angle of incidence at the curved top interface and is trapped inside the Si material. The light remains trapped until it either absorbed or scattered back into the escape wedge for the two-dimensional structure.[41–43] Consequently, the lens array curved surface structure results in the increase of absorptivity within the PV Si layer. For the milimeter-sized cylindrical lens array concentrator used, the focusing effect of supporting layer height on absorptivity is shown in Fig. 6(b). It is found form Fig. 6(b) that h has an important effect on the absorptivity of Si solar cells with the array concentrator. The calculated maximum value of $A_{\rm int}$ is equal to 61.79% at $h = 3.5$ mm in Fig. 6(b), which is increased by 11% larger than that of the device without the array concentrator.

The spatially resolved carrier generation rate $G(\boldsymbol{r})$ (Eq. (2)) obtained by the ray-tracing simulation is considered as a light source in the FEM charge simulation. Figure 7(a) shows the simulated current density–voltage curves and PCEs for two Si solar cells with and without the CLAC, respectively. It is noted that the values of $J_{\rm sc}$, FF, and PCE obtained by theoretical simulation are larger than experimental measurements, which is because the parasitic resistance, defects in Si, and absorption in ERP are not considered in the theoretical simulations. It is found from Fig. 7 that compared with the PCE of the solar cell without the CLAC, the PCE of the solar cell with the CLAC are improved by 6.3% in theory, which is close to 7.5% obtained from experiment. The tendence of PCE improvement with the supporting layer height h in Fig. 7(b) is similar to the experimental curve shown in Fig. 4. The non-monotonic behavior of the PCE improvement with h can be explained as follows. For a whole concentration solar cell,[44] its PCE increases with concentration ratio (X) and the increment of PCE improvement can be expressed as[39]

$$\Delta\eta = \frac{mk_{\rm B}T}{qV_{\rm oc}(1)}\ln X, \tag{3}$$

where $V_{\rm oc}(1)$ is the open-circuit voltage at $X = 1$. For the studied local distributed concentrating solar cell encapsulated by an ERP cylindrical array concentrator, however, there exist the focusing high-intensity region and nonfocusing low-intensity and/or shade region. The change in h affects the PCE by simultaneously changing two factors: (i) the concentration ratio X and (ii) the ratio between the light highly focused area and lower-intensity or shade area.[31,40] Larger X implies the higher efficiency in highly focused area, but in unfocused low-intensity area, the efficiency becomes lower. Therefore, for the studied solar cells with cylindrical array concentrator, it is necessary to have a delicate balance between light focusing intensity and focusing area ratio by changing the height of h. An aggressive approach to improve one of them may lead to reducing the device PCE without a proper value of h. Figures 4 and 7(b) show that the balance point is close to $h = 3.75$ mm with a focusing area ratio of 29.38%, at which the PCE reaches its maximum value.

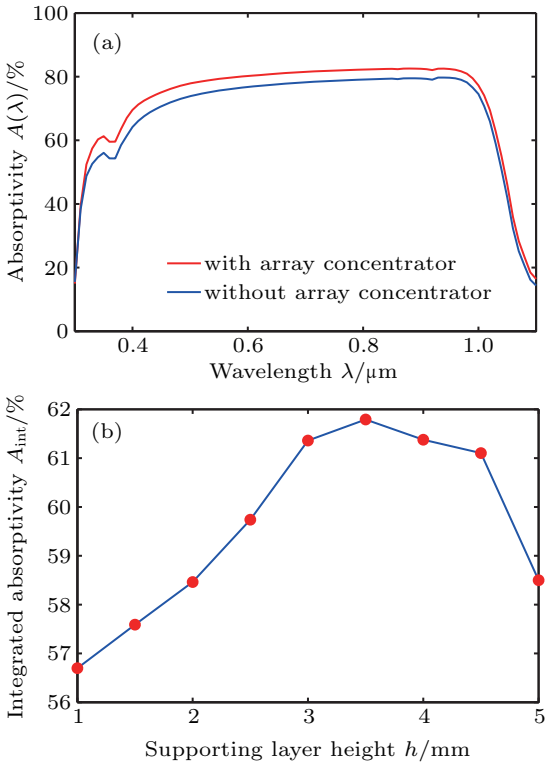


Fig. 6. (color online) (a) Absorptivity spectra of simulated solar cells with and without the array concentrator at $\theta = 0^\circ$ and $h = 2$ mm. (b) Dependence of integrated absorptivity on height of supporting layer between array contentrator and surface of bare Si solar cell at $\theta = 0^\circ$.

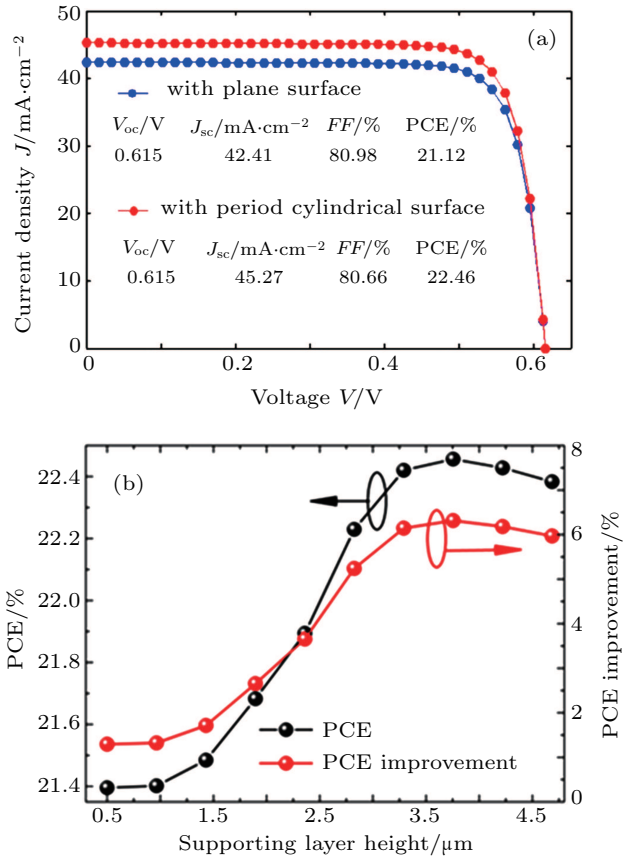


Fig. 7. (color online) FEM simulations of electrical performance of Si solar cells with and without a cylindrical array concentrator. (a) *J*–*V* curves of solar cells under normal incidence and $h = 3.75$ mm, where table in inset shows electrical parameters of solar cells. (b) Plots of PCE of solar cell with an ERP array concentrator and its PCE improvement relative to the solar cell with a plane ERP surface versus supporting layer height.

4. Conclusion

A millimeter-sized cylindrical lens array concentrator is proposed to improve the PCE of silicon solar cells. We have both theoretically and experimentally investigated the absorption enhancement and PCE improvement of silicon solar cells with the millimeter-sized cylindrical ERP lens array concentrator fabricated by a simple and well-engineered soft imprint technique. The simulation and measurement results show that the PCE of silicon solar cell with the ERP cylindrical array concentrator is dependent on the supporting layer height and the optimal supporting layer height is equal to 3.75 mm, at which the PCE reaches its maximum value. Intriguingly, it is discovered that the averaged PCE over the incident angle range of 0°–60° is improved by 10%, compared with the averaged PCE of the solar cell without the concentrator. It should be pointed out that milli-scale lens arrays, unlike micro- and/or nano-scale microlens arrays which are fabricated by costly and complicated photo lithography or electron beam direct writing system, can be obtained conveniently by simple equipment and technique. Furthermore, the millimeter-sized lens array AR coating facilitates cleaning the solar cells when they are installed outdoor. In a word, this work provides a way to design and fabricate simple, practical, and mass-production optical trapping structures of high-efficiency solar cells.

References

[1] Asim N, Sopian K, Ahmadi S, Saeedfar K, Alghoul M A, Saadatian O and Zaidi S H 2012 *Renew. Sust. Energy Rev.* **16** 5834
[2] Green M A, Emery K, Hishikawa Y, Warta W and Dunlop E D 2015 *Prog. Photovolt. Res. Appl.* **23** 1
[3] Kannan N and Vakeesan D 2016 *Renew. Sust. Energy Rev.* **62** 1092
[4] Mohammed T I, Koh S C L, Reaney I M, Acquaye A, Schileo G, Mustapha K B and Greenough R 2017 *Renew. Sust. Energy Rev.* **80** 1321
[5] Chen W H and Hong C N 2016 *Sol. Energy Mater. Sol. Cells* **157** 48
[6] Papet P, Nichiporuk O, Kaminski A, Rozier Y, Kraiem J, Lelievre J F, Chaumartin A, Fave A and Lemiti M 2006 *Sol. Energy Mater. Sol. Cells* **90** 2319
[7] Haase C and Stiebig H 2007 *Appl. Phys. Lett.* **91** 061116
[8] Jiang Y, Shen H L, Pu T, Zheng C F, Tang Q T, Gao K, Wu J, Rui C B, Li Y F and Liu Y W 2017 *Sol. Energy* **142** 91
[9] Stapf A, Honeit F, Gondek C and Kroke E 2017 *Sol. Energy Mater. Sol. Cells* **159** 112
[10] Phillips B M, Jiang P and Jiang B 2011 *Appl. Phys. Lett.* **99** 191103
[11] Chong T K, Wilson J, Mokkapati S and Catchpole K R 2012 *J. Optics* **14** 024012
[12] Esteban R, Laroche M and Greffet J J 2010 *Appl. Phys. Lett.* **97** 221111
[13] Jia Z H, Cheng Q, Song J, Si M T and Luo Z X 2016 *Opt. Commun.* **376** 14
[14] Kanamori Y, Hane K, Sai H and Yugami H 2001 *Appl. Phys. Lett.* **78** 142
[15] Huang B R, Yang Y K, Lin T C and Yang W L 2012 *Sol. Energy Mater. Sol. Cells* **98** 357
[16] Jung J Y, Guo Z Y, Jee S W, Um H D, Park K T and Lee J H 2010 *Opt. Express* **18** A286
[17] Michael D K, Shannon W B, Jan A P, Daniel B T E, Morgan C P, Emily L W, Joshua M S, Ryan M B, Nathan S L and Harry A A 2010 *Nat. Mater.* **9** 239
[18] Rahul D, Marko M, Rodrigo N, Sujay P, Alberto S and Dietmar K 2009 *Opt. Express* **17** 23058
[19] Xi Z Q, Yang D R, Dan W, Jun C, Lia X H and Que D L 2004 *Renew. Energy* **29** 2101
[20] Zhong S, Huang Z, Lin X, Zeng Y, Ma Y and Shen W 2015 *Adv. Mater.* **27** 555
[21] Goetzberger A, Knobloch J and Voss B 1998 *Crystalline Silicon Solar Cells* (Chichester: John Wiley & Sons)
[22] Poulek V, Strebkov D S, Persic I S and Libra M 2012 *Sol. Energy* **86** 3103
[23] Pern F J and Glick S H 1997 *AIP Conf. Proc.* **394** 811
[24] Tao W and Du Y 2015 *Sol. Energy* **122** 718
[25] Dubey R S, Jhansirani K and Singh S 2017 *Results Phys.* **7** 77
[26] Leem J W, Guan X Y, Choi M and Yu J S 2015 *Sol. Energy Mater. Sol. Cells* **134** 45
[27] Amalathas A P and Alkaisi M M 2017 *Mater. Sci. Semicond. Proc.* **57** 54
[28] Raut H K, Nair A S, Dinachali S S, Ganesh V A, Walsh T M and Ramakrishna S 2013 *Sol. Energy Mater. Sol. Cells* **111** 9
[29] Sánchez-Illescas P J, Carpena P, Bernaola-Galván P, Sidrach-De-Cardona M, Coronado A V and álvarez J L 2008 *Sol. Energy Mater. Sol. Cells* **92** 323
[30] Ghazi S, Sayigh A and Ip K 2014 *Renew. Sust. Energy Rev.* **33** 742
[31] Ha S H, Yu H W, Jang N S, Kim J H, Kim S H and Kim J M 2016 *Sol. Energy Mater. Sol. Cells* **155** 362
[32] Fan H B and Yuen M M F 2007 *Polymer* **48** 2174
[33] Nogi M, Handa K, Nakagaito A N and Yano H 2005 *Appl. Phys. Lett.* **87** 243110
[34] Lin J, Chen M, Ke Y, Ren C, Xu Z, Zhang Y and Fang C 2018 *Chin. Phys. B* **27** 018802

[35] Tseng J K, Chen Y J, Pan C T, Wu T T and Chung M H 2011 *Sol. Energy* **85** 2167

[36] 2017 PVLighthouse Web https://www2.pvlighthouse.com.au/Resources/Photovoltaic%20materials

[37] Zhang Y J, Zheng J, Zhao X S, Ruan X K, Cui G H, Zhu H Y and Dai Y X 2018 *Opt. Commun.* **410** 369

[38] Maryasin V, Bucci D, Rafhay Q, Panicco F, Michallon J and Ccachopo A K 2017 *Sol. Energy Mater. Sol. Cells* **172** 314

[39] Nelson J 2003 *The Physics of Solar Cells* (London: Imperial College Press)

[40] Price J S, Sheng X, Meulblok B M, Rogers J A and Giebink N C 2015 *Nat. Commun.* **6** 6223

[41] Miller O D, Yablonovitch E and Kurtz S R 2012 *IEEE J. Photovolt.* **2** 303

[42] Tiedje T, Yablonovitch E, Cody G D and Brooks B G 1984 *IEEE T. Electron Dev.* **ED-31** 711

[43] Yablonovitch E and Cody G D 1982 *IEEE T. Electron Dev.* **ED-29** 300

[44] Paternoster G, Zanuccoli M, Bellutti P, Ferrario L, Ficorella F, Fiegna C, Magnone P, Mattedi F and Sangiorgi E 2015 *Sol. Energy Mater. Sol. Cells* **134** 40